JOURNAL OF AGRICULTURAL AND FOOD CHEMISTRY

pubs.acs.org/JAFC Article

D-Pinitol Improves Diabetic Sarcopenia by Regulation of the Gut Microbiome, Metabolome, and Proteome in STZ-Induced SAMP8 Mice

Xin Yu, Pei Li, Baoying Li, Fei Yu, Wenqian Zhao, Xue Wang, Yajuan Wang, Haiqing Gao, Mei Cheng,* and Xiaoli Li*

Cite This: https://doi.org/10.1021/acs.jafc.4c03929 Read Online

ACCESS | Metrics & More | Article Recommendations | Supporting Information

ABSTRACT: D-Pinitol (DP) is primarily found in *Vigna sinensis*, which has been shown to have hypoglycemic and protective effects on target organs. However, the mechanism of DP in treating diabetic sarcopenia (DS) is still unclear. To explore the underlying mechanism of DS and the protective targets of DP by high-throughput analysis of 16S rRNA gene, metabolome, and the proteome. Streptozotocin-induced SAMP8 mice were intragastrically administrated DP (150 mg/kg) for 8 weeks. Fecal 16S rRNA gene sequencing and gastrocnemius muscle metabolomic and proteomic analyses were completed to investigate the gut−muscle axis interactions. DP significantly alleviated the muscle atrophy in diabetic mice. Dysfunction of the gut microbiota was observed in the DS mice. DP significantly reduced the Parabacteroides, Akkermansia, and Enterobacteriaceae, while it increased Lachnospiraceae_NK4A136. Metabolome and proteome revealed that 261 metabolites and 626 proteins were significantly changed in the gastrocnemius muscle of diabetic mice. Among these, DP treatment restored 44 metabolites and 17 proteins to normal levels. Functional signaling pathways of DP-treated diabetic mice included nucleotide metabolism, β-alanine, histidine metabolism, ABC transporters, and the calcium signaling pathway. We systematically explored the molecular mechanism of DS and the protective effect of DP, providing new insights that may advance the treatment of sarcopenia.

KEYWORDS: *D-pinitol, diabetic sarcopenia, gut microbiota, metabolome, proteome*

1. INTRODUCTION

Sarcopenia, significantly influenced by diabetes mellitus, is characterized by muscle atrophy, muscle strength, and function decline.[1] Diabetic sarcopenia (DS), considered as a complication of diabetes, leads to an increased risk of falls, fractures, physical disabilities, and even mortality. The condition severely impacts the quality of life for those diabetic patients and escalates the economic burden on the country, society, and families.[2] Numerous studies have identified hyperglycemia, insulin resistance, oxidative stress, and inflammation as pivotal factors in the development and progression of DS.[3,4] The precise molecular mechanisms underlying DS are complex and need further exploration. Therefore, elucidating the molecular mechanisms and searching for effective therapeutic drug targets hold considerable clinical significance.

At present, the treatment of DS has primarily centered on nutrition and exercise interventions. Additionally, multiple hypoglycemic drugs have proven effective in treating diabetes mellitus.[5] However, the clinical data of antidiabetic drugs on DS is still insufficient, with contradictory findings in different studies. In recent years, an array of natural compounds, including resveratrol, curcumin, geniposide, catechin, and flavonoids, have demonstrated potential in the prevention and management of sarcopenia.[6−8] Our former research found that D-pinitol (DP) had hypoglycemic activity and cardioprotective effect in diabetic mice.[9,10] DP has a wide range of plant sources in nature, mainly found in *Vigna sinensis*, soybean, and pine plants. This compound is endowed with various physiological activities, such as insulin sensitization, hypoglycemic, antioxidation, anti-inflammatory, and antitumor effects, among others. Emerging evidence suggests that DP could improve postprandial hyperglycemia and insulin sensitivity in patients with type 2 diabetes.[11,12] Zhang et al. reported that extract of ice plant (main component DP) modulated gut microbiota composition and attenuated hyperglycemia in diabetic GK rats.[13] However, the molecular mechanisms of DP in treating diabetes, especially DS, remain elusive.

The gut−muscle axis is believed to be a micronutrient and metabolites derived from the gut microbiota can modulate muscle function and mass.[14] Recent investigations have unveiled a significant correlation between gut microbiota and sarcopenia, which plays a crucial role in the maintenance of skeletal muscle homeostasis. It has been reported that gut microbiota affects muscle protein synthesis by regulating the host's inflammatory response, oxidative stress, mitochondrial function, nutrient absorption and hormone levels.[15−17] More-

Received: May 6, 2024
Revised: June 4, 2024
Accepted: June 7, 2024

over, gut microbiota plays an important part in the pathogenesis of diabetes.[18] Therefore, gut microbiota emerge as an important factor in the pathogenesis of DS. However, the intrinsic mechanisms of the gut−muscle axis in DS remain elusive.

With the development of multiomics technology and bioinformatics analysis, microbiome integrated with metabolome and proteome can now be used to better understand the gut microbial community and the mechanisms of sarcopenia.[19] Gene Ontology (GO) and Kyoto Encyclopedia of Genes and Genomes (KEGG) pathway enrichment analyses were used to predict the molecular mechanism of DP and provide comprehensive insight into its biological functions and associated biochemical pathways. By employing 16S rRNA gene sequencing to characterize gut microbiota, in conjunction with nontargeted metabolomic profiling and TMT proteomic analysis of the gastrocnemius muscle, this study endeavors to elucidate the potential mechanisms of DS and targets of DP. The data were analyzed through advanced bioinformatics to establish the cross-sectional framework of gut−muscle axis and provide a beneficial approach of new therapies for sarcopenia.

2. MATERIALS AND METHODS

2.1. Materials. Streptozotocin (STZ) and D-pinitol (purity 95%, lot no.: BCCB9551) were supplied by Sigma-Aldrich (St. Louis, USA). TMT 10 plex kit was obtained from Thermo Scientific (Carlsbad, USA). The antibodies were described in Supporting Information (SI) Table 1. All additional chemical reagents were purchased as analytical grade.

2.2. Animals and Groups. The Supporting Information contained detailed procedure descriptions. R1 (n = 10): control SAMR1 group; CC (n = 10): control SAMP8 group, DM (n = 12): STZ-induced SAMP8 group, and DP (n = 12): DP treated STZ-induced SAMP8 group. The Shandong University Animal Ethics Committee gave its approval to all procedures (approval no.: 21170). All animal trials followed the Experimental Animal Center of Shandong University's protocols and the ARRIVE guidelines. At the end of the experiments, all animals were starved overnight and killed under sodium pentobarbital anesthesia. Fasting blood and cecal contents were obtained, and the gastrocnemius muscles were dissected. The samples were maintained at −80 °C until further examination.

2.3. Grip Strength, Rota-rod Tests, and Body Composition Measurement. Forepaws grip strength, coordination, and balance of mice was determined with a force gauge and rota-rod apparatus (Yiyan Technology Development, Jinan, China). Mice caught by tail grasped the grid connected to the force gauge with its forepaws. Mice were pulled until they released their forepaws from the grid. After three repeats, the average value of the grip strength (g) was recorded. Mice were trained for 3 days. The acceleration settings were 40 rpm, and the running time (latency to fall, S) until the first fell off was recorded for three testing periods. Lean mass, bone mineral density (BMD), and fat mass were measured with an XR-800 dual-energy X-ray absorptiometry (Norland, USA).

2.4. Estimation of Body Weight (BW), Gastrocnemius Weight (GW)/BW, GW/Tibia Length (TL), and Fasting Blood Glucose (FBG). Mice and gastrocnemius were weighed at the end of the experiment. The ratios of GW/BW (mg/g) and GW/TL (mg/mm) were computed by using TL measurements. Serum FBG levels were measured using an Automatic Biochemistry and Analysis Instrument (Bayer, Germany).

2.5. Light Microscopy. The gastrocnemius was removed, preserved in 4% paraformaldehyde, embedded in paraffin, and sectioned into 4 μm thick pieces. Hematoxylin and eosin (HE) staining was performed.

2.6. 16s rRNA Gene Sequencing. The OMEGA Soil DNA Kit (Omega Bio-Tek, Norcross, USA) was used to extract microbial DNA from cecal content samples (n = 9 for each group, CC, DM, and DP), in accordance with the manufacturer's instructions. The quantity and quality of DNAs were measured using a NanoDrop NC 2000 spectrophotometer (Thermo Fisher Scientific, USA) and agarose gel electrophoresis. The 16S rRNA gene's variable V3−V4 regions were amplified using a bacterial universal primer pair (338F and 806R). The Illumina MiSeq system (Illumina MiSeq, USA) was used to determine the sequencing. Raw sequencing data were mainly performed with QIIME 2 (version 2019.4).

2.7. Nontargeted Metabolomic Analysis of Gastrocnemius Tissue. Gastrocnemius tissues (n = 9 each group, CC, DM, and DP) were selected to extract metabolites. Then 200 μL of precold water, 800 μL of precooled methanol acetonitrile, and 20 mg of each sample were added and thoroughly mixed. Using a high-speed vacuum concentration centrifuge, we evaporated the supernatant is evaporated. HILIC column and Shimadzu-LC30 ultra high-performance liquid chromatography (UHPLC) were used to separate the sample. Positive and negative ion modes were used for the ESI-MS investigations, respectively. The main steps include sample collection, metabolite extraction, QC preparation, LC-MS/MS mass spectrometry, and data analysis. More detailed methods are described in the Supporting Information.

2.8. TMT-Labeled Quantitative Proteomic Analysis of Gastrocnemius Tissue. Proteins were extracted from gastrocnemius tissues (n = 9 in each group: CC, DM, and DP). Then three samples of each group were mixed into a pool. SDT was used to lyse the gastrocnemius tissue, and the BCA method was used to quantify the results. TMT reagent was applied to label the digested samples in accordance with the kit's instructions. The Q Exactive HF-X mass spectrometer coupled with an Easy nLC 1200 (Thermo Fisher Scientific) was carried out. The main steps include sample preparation, TMT peptide labeling and peptide grading, LC-MS/MS analysis, database retrieval, and statistic methods.[20] More information was described in the Supporting Information.

2.9. Integrated Analysis of Between Microbiome and Metabolome and Between Metabolome and Proteome. The correlation and molecular interaction networks of differential microbes and metabolites were analyzed using R (version: 4.0.5) and Cytoscape 3.8.2. Additionally, Cytoscape 3.8.2 and R (version: 4.0.5) were utilized to examine the molecular interaction networks and considerably enhanced KEGG pathways of differentially expressed metabolites and proteins.

2.10. Western Blot Analysis. The samples of gastrocnemius were homogenized in PMSF-containing ice-cold lysis buffer (Beyotime Biotechnology, Jiangsu, China). A similar quantity of protein was separated using 10% SDS-PAGE and then put onto membranes made of polyvinylidene difluoride. After sealing the membrane with either PBST-5% skim milk or PBST-5% BSA, the antibody was incubated at 4 °C for the whole night as follows: ADP ribosylation factor-like GTPase 6 interacting protein 5 (Arl6ip5, 1:1000), sorting nexins 6 (SNX 6, 1:5000), and tripartite motif containing protein 54 (Trim54, 1:1000). An hour was spent at room temperature by applying the secondary antibody (1:1000). The immunoblot band intensity was calibrated by using β-actin (1:2000) as the reference. Densitometry was used to quantify each detected protein band, and ImageJ densitometry software was used for analysis.

2.11. Statistical Analysis. Data were expressed in the form of mean ± SD. One-way analysis of variance (ANOVA) was used for the statistical analysis between the groups, and Tukey's HSD test was used for multiple comparisons. To identify various genera of bacteria, metagenomeSeq analysis and linear discriminant analysis effect size (LEfSe) were employed. With Fisher's exact test, GO and KEGG enrichment analyses were carried out. A P-value of less than 0.05 was deemed statistically noteworthy. Version 22.0 of SPSS for Windows was used for all analyses (SPSS, Chicago, USA).

3. RESULTS

3.1. Effects of DP on BW, Grip Strength, and Latency to Fall, GW/BW, GW/TL, and FBG. At the end of the

https://doi.org/10.1021/acs.jafc.4c03929
J. Agric. Food Chem. XXXX, XXX, XXX−XXX

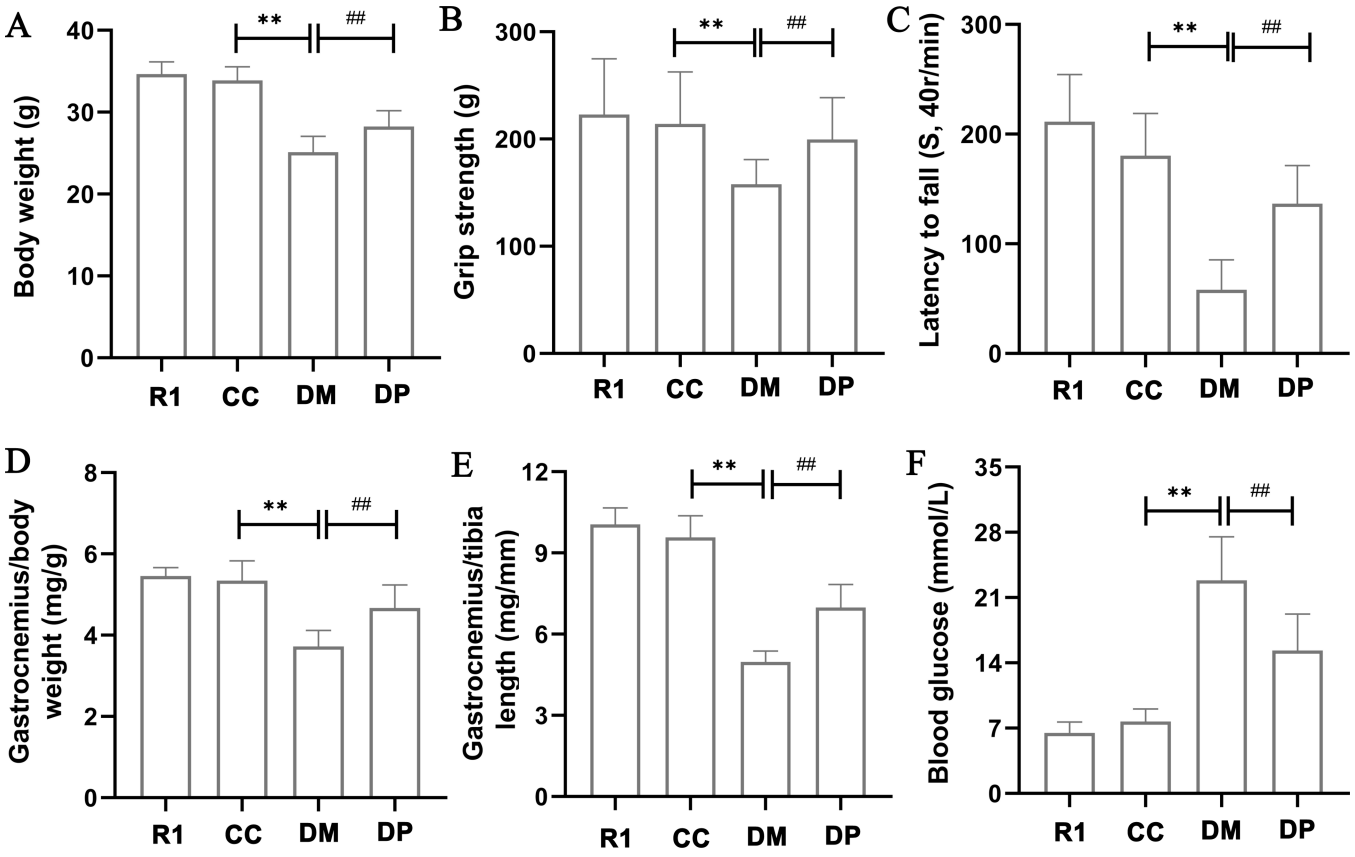

Figure 1. Effects of DP on BW, grip strength, and latency to fall, GW/BW, GW/TL, and FBG in STZ induced SAMP8 mice. (A) Body weight changes of the mice. (B) Grip strength changes of the mice. (C) Latency to fall changes of the mice. (D) GW/BW changes of the mice. (E) GW/TL changes of the mice. (F) Serum FBG changes of the mice. *$P < 0.05$, **$P < 0.01$ compared with CC group; $^{\#}P < 0.05$, $^{\#\#}P < 0.01$ compared with DM group. R1, control SAMR1 group; CC, control SAMP8 group; DM, STZ induced SAMP8 group; DP, DP treated STZ induced SAMP8 group. DP, D-pinitol; BW, body weight; GW, gastrocnemius weight; TL, tibia length; FBG, fasting blood glucose; STZ, streptozotocin.

experiment, the survival numbers for the R1 group, CC group, DM group, and DP group were 10, 10, 10, and 11, respectively. The BW, grip strength, and latency to fall, GW/BW, and GW/TL of the DM group were significantly lower than those in the CC group, while DP significantly increased them ($P < 0.01$, Figure 1A−E). FBG of mice showed a significant increase in the DM group ($P < 0.01$), while DP significantly decreased the FBG of diabetic mice ($P < 0.01$, Figure 1F).

3.2. Effects of DP on Lean Mass, Fat Mass, BMD, and Gastrocnemius Histological Findings. The lean mass, fat mass, BMD of mice showed a significant decrease in the DM group compared with CC group ($P < 0.01$). However, DP treatment, the lean mass and BMD were significantly improved in the diabetic mice ($P < 0.01$, Figure 2A−C). Under light microscopy, skeletal muscles showed smaller fiber size and myofibers cross-sectional area (CSA) in diabetic mice, which were improved by DP treatment ($P < 0.01$, Figure 2D,E).

3.3. Effects of DP on Gut Microbiota Diversity Analysis and Composition. The α-diversity indexes have Chao 1, Simpson, Shannon, Pielou_e, Observed_species, Faith_pd, and Goods_coverage. The richness and diversity of diabetic mice were lower than those in the CC group. DP improved the richness and diversity (Figure 3A). Moreover, the overall structure of gut microbiota obtained through Jaccard based PCoA indicates that clear separation was showed in the CC, DM, and DP groups (Figure 3B). Based on univariate analysis, the composition of gut microbiota was analyzed at the phylum, class, order, family, and genus levels (Figure 3C−G).

3.4. Effects of DP on Gut Microbiota Species. Microbiomics analysis showed that 689 amplicon sequence variants (ASVs) had significantly changed between the DM group and CC group. Among these, DP treatment restored 110 differential ASVs to normal levels (Figure 4A, and SI, Table 2). The clustering heatmap showed significantly altered genus levels in the combined data sets. Genus levels plotted based on log-transformed fold change in abundance between DM group and CC group (Figure 4B), between the DP group and DM group (Figure 4C).

The linear discriminant analysis effect size and cladogram displaying differentially abundant taxonomic clade analysis were compared with between DM group and CC group (Figure 4D,F), and between DP group and DM group (Figure 4E,G). Dysfunction of gut microbiota was found in the diabetic mice, such as increase in Parabacteroides, Akkermansia, and Enterobacteriaceae, and decrease in Lachnospiraceae_NK4A136 ($P < 0.01$). DP significantly reduced the Parabacteroides, Akkermansia, and Enterobacteriaceae, while increased Lachnospiraceae_NK4A136 in DP group ($P < 0.01$, Figure 4H).

3.5. Metabolites Identification and Potential Targets of DP in Treating DS. Principal component analysis (PCA), orthogonal partial least-squares discriminant analysis (OPLS-DA), and permutation tests were performed to further filter out differential metabolites in positive and negative ion mode

https://doi.org/10.1021/acs.jafc.4c03929
J. Agric. Food Chem. XXXX, XXX, XXX−XXX

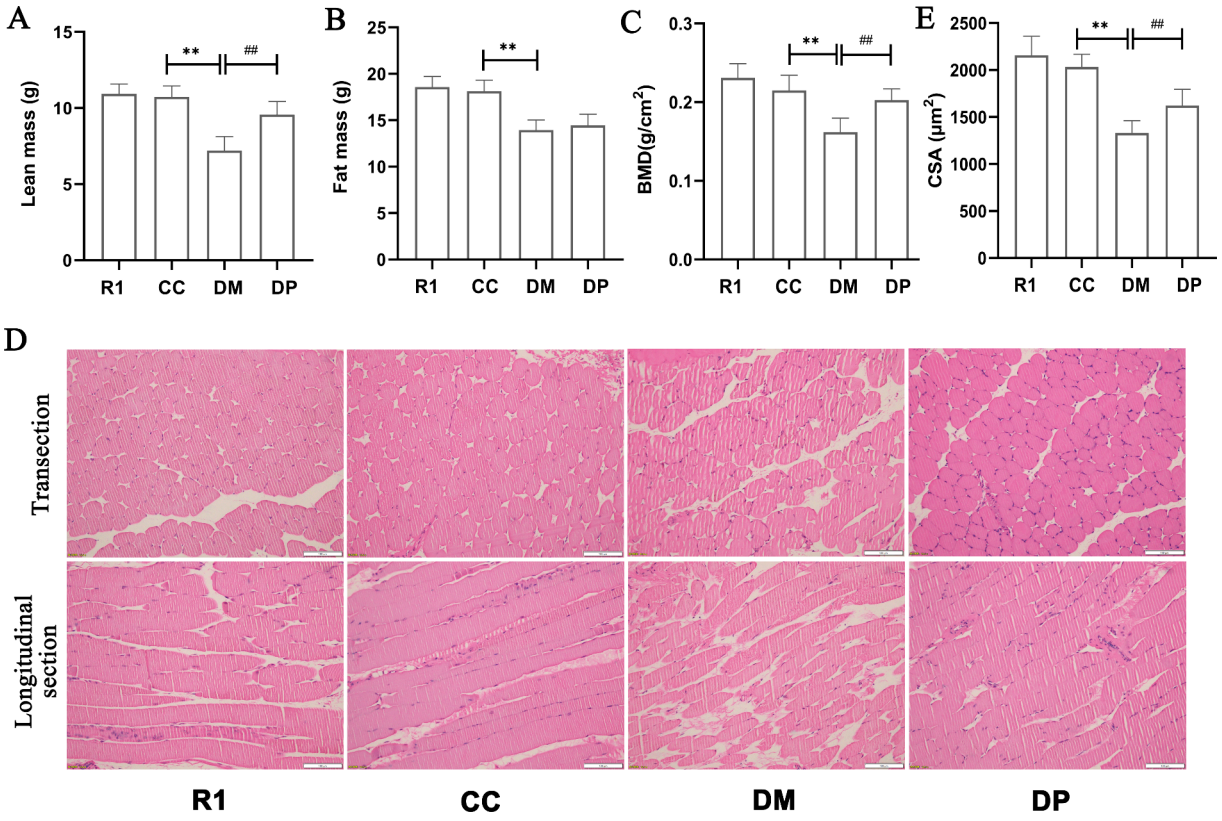

Figure 2. Effects of DP on lean mass, fat mass, BMD, and gastrocnemius histological findings. (A) Lean mass changes of the mice. (B) Fat mass changes of the mice. (C) BMD changes of the mice. (D) Representative light micrographs of the heart (HE, bar: 100 μm). (E) Myofibers CSA changes of the mice. $^{*}P < 0.05$, $^{**}P < 0.01$ compared with CC group; $^{\#}P < 0.05$, $^{\#\#}P < 0.01$ compared with DM group. R1, control SAMR1 group; CC, control SAMP8 group; DM, STZ induced SAMP8 group; DP, DP treated STZ induced SAMP8 group. DP, D-pinitol; BMD, bone mineral density; CSA, cross-sectional area.

of CC group, DM group, and DP group (SI, Figure 1; Figure 5A,B). Metabolomics analysis showed that 261 differentially regulated metabolites (DRMs) had significantly changed between DM group and CC group. Among these, DP treatment restored 44 metabolites to normal levels (Figure 5C, and SI, Table 3). The back-regulated metabolites include carnosine, histidine (His), uridine 5′-monophosphate (5′-UMP), cytidine 5′-monophosphate (5′-CMP), D-carnitine, α-aminoadipate, 4-hydroxy-6-methylpyran-2-one, and 5,7-dihydroxyflavanone. Volcano plot and cluster heatmap showed significantly altered metabolites in the combined data set. Metabolites plotted for log-transformed fold change in abundance between DM group and CC group (Figure 5D,F), between DP group and DM group (Figure 5E,G).

KEGG signaling pathways in the DM group are shown in Figure 5H and SI, Table 4. The signaling pathways mainly include ABC transporters, mTOR, FoxO, AMPK, and CAMP signaling pathway, nucleotide, His, purine, and β-alanine metabolism. KEGG signaling pathways in the DP group were shown in Figure 5I and SI, Table 5. The signaling pathways mainly include ABC transporters, nucleotide, His, pyrimidine, and β-alanine metabolism.

3.6. Protein Identification and Potential Targets of DP Therapy for DS. PCA plots for the proteomics are shown in SI, Figure 2. Proteomics analysis showed that 626 proteins had significantly changed between DM group and CC group. Among these, DP treatment restored 17 proteins to normal levels (Figure 6A, and SI, Table 6). The back-regulated proteins include methyltransferase-like 26 (Mettl26), peptidyl-prolyl isomerase (Fkbp1a), Arl6ip5, SNX6, and Trim54. Volcano plot and cluster heatmap showed significantly altered proteins in the combined data set. Proteins plotted for log-transformed fold change in abundance between DM group and CC group (Figure 6B,D), between DP group and DM group (Figure 6C,E).

We analyzed the biological processes (BP), cellular components (CC), and molecular functions (MF) of differentially expressed proteins (DEPs) between the CC group and DM group. The majority was involved in metabolic process and nitrogen compound metabolic process, cytoplasm, and catalytic activity (Figure 6F). The back-regulated proteins by DP treatment were involved in cytosolic calcium ion transport, sarcoplasmic reticulum membranes, and transforming growth factor beta receptor binding (Figure 6G). The subcellular localization of the DM group mainly occurred in the cytoplasm, membrane, and mitochondria (Figure 6H). The back-regulated proteins by DP treatment were mainly located in the cytoplasm, membrane, and endoplasmic reticulum (Figure 6I).

3.7. KEGG Pathway Enrichment and PPI Network Analysis, Validation of DP Targets of Proteome with Western Blot. KEGG signaling pathways analyzed DM groups and proteins treated with DP (Figure 7A,B; SI, Tables 7 and 8). KEGG signaling pathways in the DM group mainly include focal adhesion, amino acids, and aminoacyl-tRNA biosynthesis, metabolic, and PPAR signaling pathways. KEGG signaling pathways in the DP group mainly include calcium signaling pathway, GnRH signaling pathway, and GABAergic

https://doi.org/10.1021/acs.jafc.4c03929
J. Agric. Food Chem. XXXX, XXX, XXX−XXX

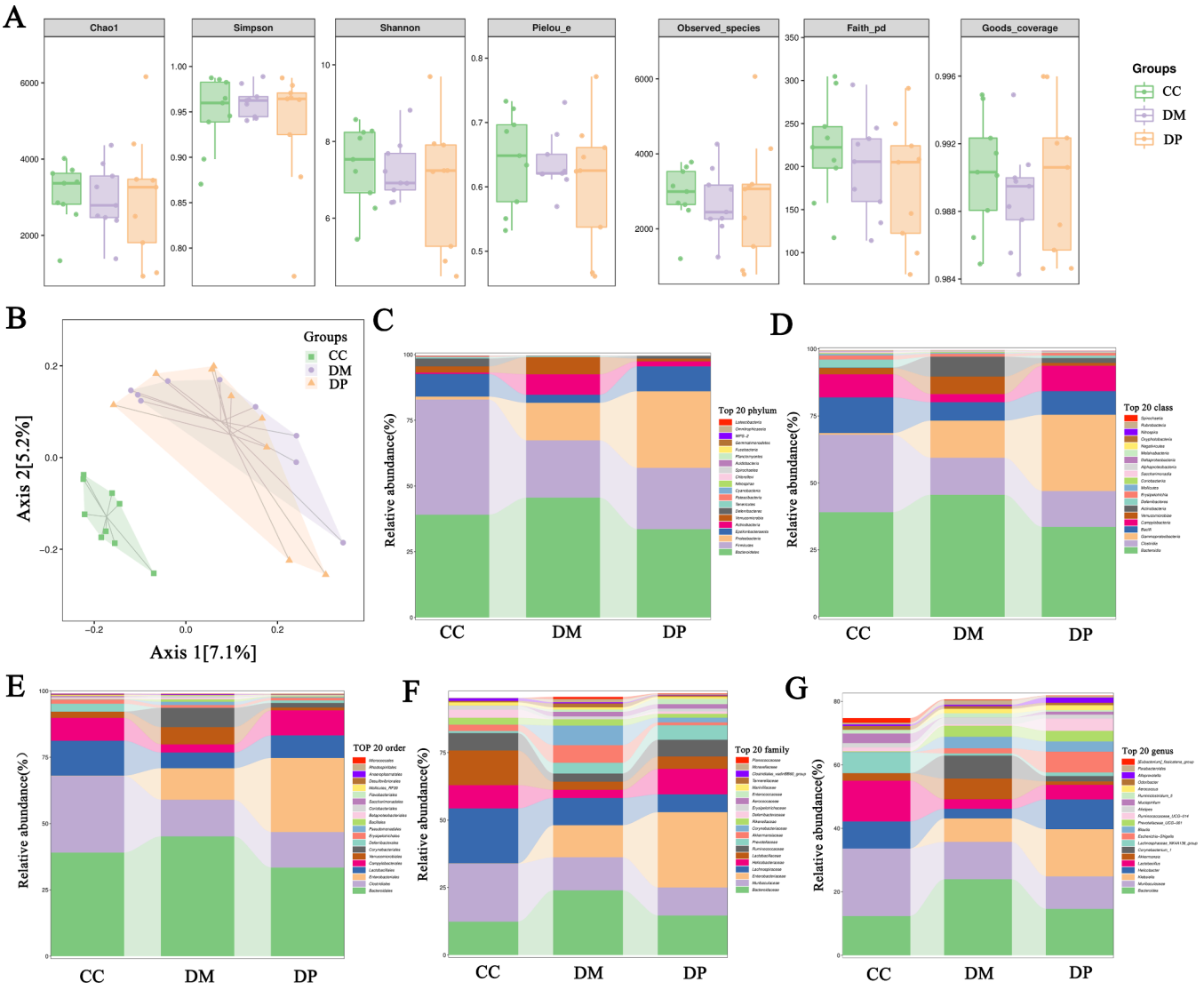

Figure 3. Effects of DP on gut microbiota diversity analysis and composition in the diabetic mice. (A) Alpha diversity indexes (Chao 1, Simpson, Shannon, Pielou_e, Observed_species, Faith_pd, and Goods_coverage indexes). (B) Jaccard PCoA analysis of gut microbiota based on the ASV data. (C–G) Composition of gut microbiota at phylum, class, order, family, and genus levels. ASV, amplicon sequence variant; DP, D-pinitol.

synapse. PPI pathway–gene and pathway–pathway network analyzed DEPs between DM group and CC group and between DP group and DM group (Figure 7C–F). PPI pathway-gene networks by DP treatment were related to calcium signaling pathway, and GnRH signaling pathway.

Compared to the CC group, the protein expression of Arl6ip5 and SNX6 was up-regulated, while the expression of Trim54 was down-regulated in the gastrocnemius tissues of the DM group. DP could inhibit Arl6ip5 and SNX6 expression and increased Trim54 expression ($P < 0.01$, Figure 7G–J).

3.8. Associations Between Gut Microbiome and Gastrocnemius Metabolome and Proteome. We further validated the possible interaction between the gut microbiome and host gastrocnemius metabolome by analyzing the correlation between the two data. Spearman correlation analysis between gut microbiota and metabolites revealed several significant associations in the DM group and DP group. Correlation coefficient matrix heatmap, hierarchical clustering heatmap, and network diagram between DM group and CC group, between DP group and DM group (SI, Figure 3). The increase in abundance of Parabacteroides was mainly positively correlated with DL-β-hydroxybutyric acid, and negatively correlated with 5′-UMP, benzoic acid +1O, O-hex, and aniline-2-sulfonic acid ($r = 0.453$, $r = -0.616$, $r = -0.569$, $r = -0.569$, $P < 0.05$). The increase in abundance of Akkermansia was mainly positively correlated with 3-(*sec*-butyl)-2-hydroxy-3*H*- benzo[*E*][1,4]diazepin-5(4*H*)-one, and negatively correlated with citraconic acid, carnosine, and nonic acid ($r = 0.554$, $r = -0.703$, $r = -0.630$, $r = -606$, $P < 0.05$). The decrease in abundance of Lachnospiraceae_ UCG-006 was mainly positively correlated with aniline-2-sulfonic acid, carnosine, and 5′-CMP ($r = 0.627$, $r = 0.589$, $r = 0.469$, $P < 0.05$). The decrease in abundance of Lachnospiraceae_N-K4A136 was mainly positively correlated with carnosine and negatively correlated with dichlorophene ($r = 0.536$, $r = -0.513$, $P < 0.05$). The down-regulation of carnosine was mainly negatively correlated with Prevotellaceae_ UCG-001 and Corynebacterium_1 ($r = -0.785$, $r = -0.748$, $P < 0.05$). His was mainly negatively correlated with Robinsoniella ($r = -0.638$, $P < 0.05$). The correlation between 5′-UMP and Ruminococcaceae was significantly positive correlation ($r = 0.667$, $P < 0.05$). 5′-UMP was mainly negatively correlated

https://doi.org/10.1021/acs.jafc.4c03929
J. Agric. Food Chem. XXXX, XXX, XXX−XXX

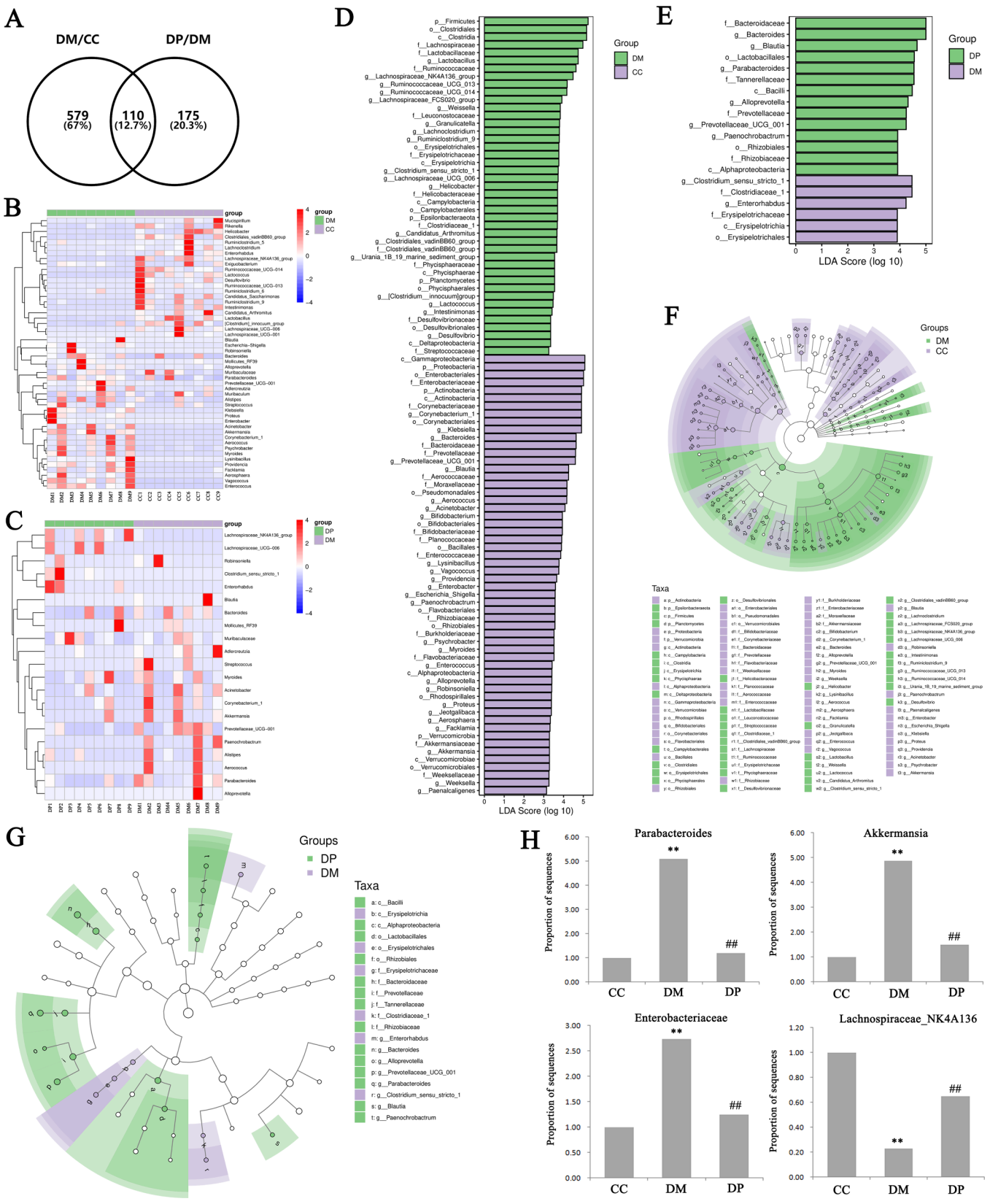

Figure 4. Effects of DP on gut microbiota species. (A) Venn analysis of ASVs. Cluster heatmap indicating significantly altered gut microbiota at genus levels: (B) between DM group and CC group, (C) between DP group and DM group. LDA scores of gut microbiota: (D) between DM group and CC group, (E) between DP group and DM group. LEfSe was used to identify the taxa with the greatest differences in gut microbiota abundance: (F) between DM group and CC group, (G) between DP group and DM group, (H) comparison of the sequences proportions of Parabacteroides, Akkermansia, Enterobacteriaceae, and Lachnospiraceae_NK4A136. *$P < 0.05$, **$P < 0.01$ compared with CC group; $^{\#}P < 0.05$, $^{\#\#}P < 0.01$ compared with DM group; CC, control SAMP8 group; DM, STZ induced SAMP8 group; DP, DP treated STZ induced SAMP8 group. DP, D-pinitol; ASV, amplicon sequence variant.

https://doi.org/10.1021/acs.jafc.4c03929
J. Agric. Food Chem. XXXX, XXX, XXX−XXX

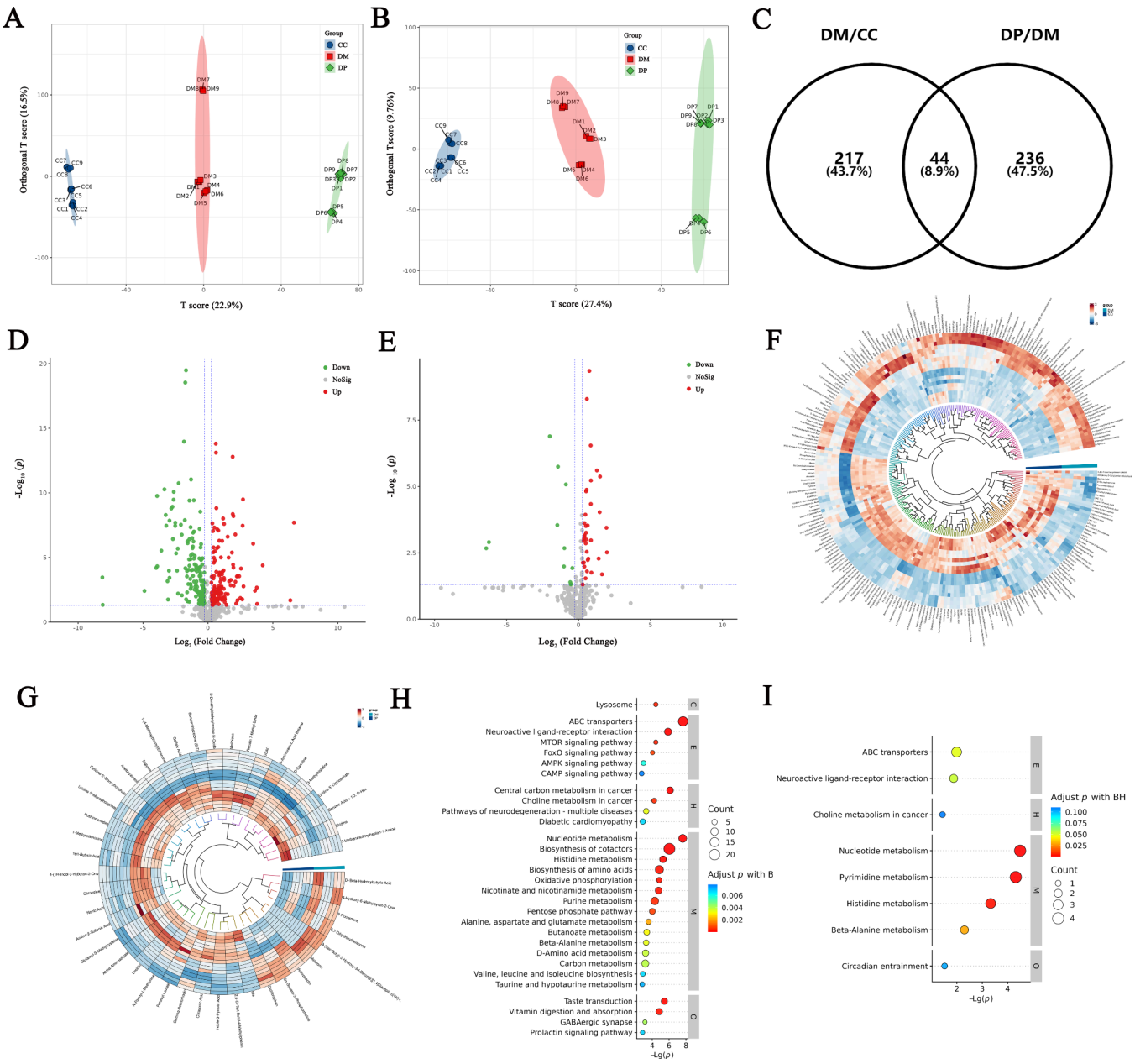

Figure 5. Metabolites identification and potential targets of DP in treating DS. OPLS-DA score plots of metabolic profiles of CC, DM, and DP groups: (A) positive ion mode, (B) negative ion mode. (C) Metabolomics analysis of 44 back-regulated metabolites after DP therapy in the gastrocnemius of diabetic mice. Volcano plot indicating significantly altered metabolites identified in the combined data sets: (D) between DM group and CC group, (E) between DP group and DM group. Cluster heatmap indicating significantly altered metabolites identified in the combined data sets: (F) between DM group and CC group, (G) between DP group and DM group. KEGG signaling pathways of differentially regulated metabolites: (H) between DM group and CC group, (I) between DP group and DM group. CC, control SAMP8 group; DM, STZ induced SAMP8 group; DP, DP treated STZ induced SAMP8 group. DP, D-pinitol.

with Robinsoniella and Corynebacterium-1 ($r = -0.693$, $r = -0.697$, $P < 0.05$). 5′-CMP was negatively correlated with Corynebacterium-1 and Paenochrobactrum ($r = -0.688$, $r = -0.673$, $P < 0.05$).

Based on 261 DRMs and 626 DEPs of the DM group, KEGG and network pathways mainly included mTOR, HIF-1, FoxO, and CAMP signaling pathway, amino, nucleotide, sugar metabolism, β-alanine, pyrimidine, alanine, aspartate, and glutamate metabolism, biosynthesis of amino acids, ABC transporters, and aminoacyl-tRNA (Figure 8A,C). Based on 44 DRMs and 17 DEPs by DP restoration, KEGG and network pathways mainly included the apelin signaling pathway, β-alanine, pyrimidine, His, and purine metabolism, ABC transporters, and glycosphingolipid biosynthesis (Figure 8B,D). Metabolic pathways between the DM group and CC group and between the DP group and DM group are shown in the Figure 8E,F.

4. DISCUSSION

The acceleration of population aging had led to an increased prevalence of DS, characterized by elevated rates of falls, functional disability, and fractures. More research spanning from basic science to clinical studies, has revealed the complexity of DS, however, no specific treatments have been

https://doi.org/10.1021/acs.jafc.4c03929
J. Agric. Food Chem. XXXX, XXX, XXX−XXX

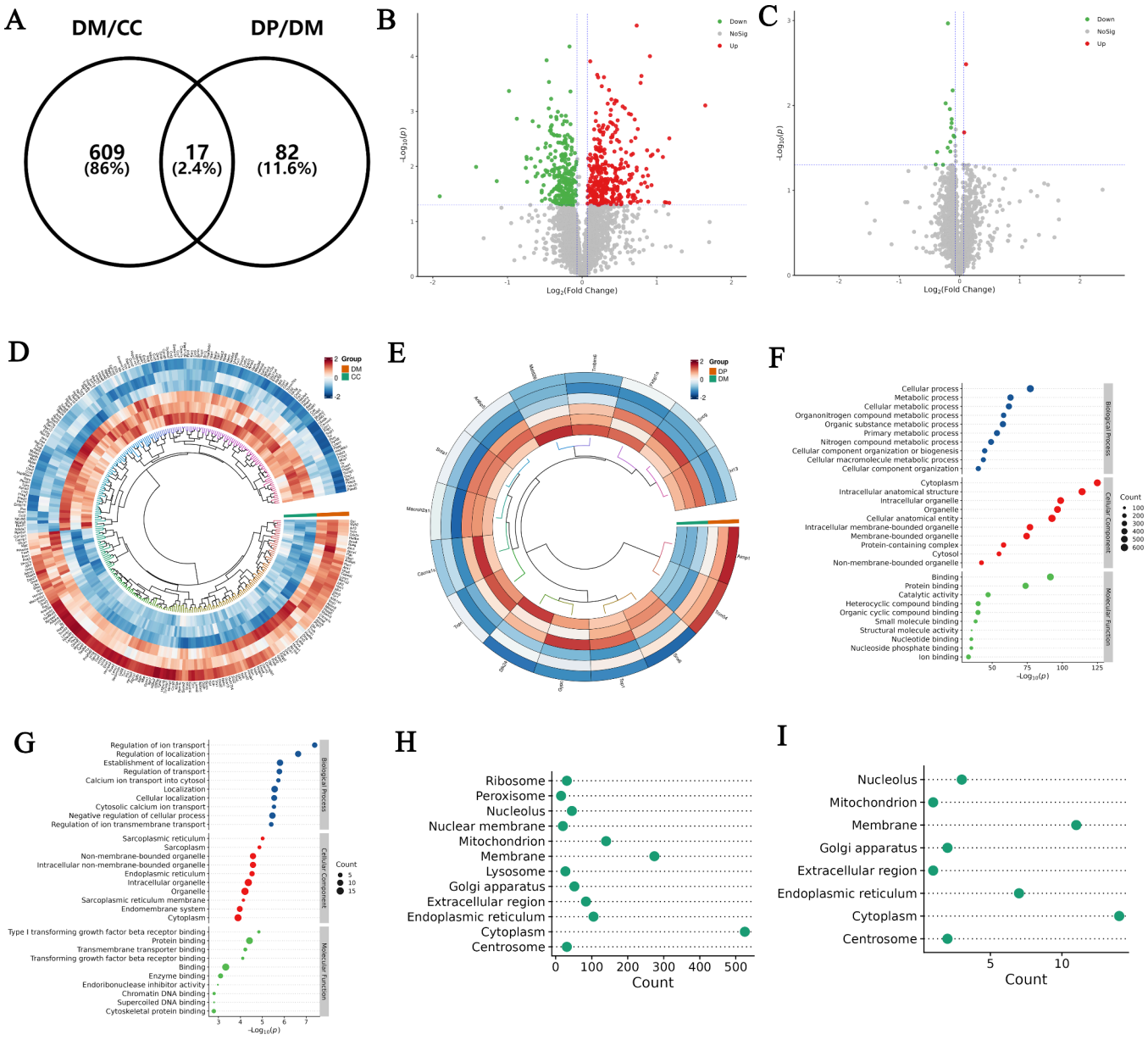

Figure 6. Protein identification and potential targets of DP in treating DS. (A) Proteomics analysis of 17 back-regulated proteins after DP therapy in the gastrocnemius of diabetic mice. Volcano plot indicating significantly altered proteins identified in the combined data sets: (B) between DM group and CC group, (C) between DP group and DM group. Cluster heatmap indicating significantly altered proteins identified in the combined data sets (D) between DP group and CC group, (E) between DP group and DM group. GO analysis of differentially expressed proteins (F) between DM group and CC group, (G) between DP group and DM group. Subcellular localization of differentially expressed proteins (H) between DM group and CC group, (I) between DP group and DM group. CC, control SAMP8 group; DM, STZ induced SAMP8 group; DP, DP treated STZ induced SAMP8 group. DP, D-pinitol.

established.[21−24] Therefore, it is crucial to identify new targets for sarcopenia, muscle mass, and function loss caused by sustained hyperglycemia. In our present study, we comprehensively investigated the interactions of gut−muscle axis by evaluating multiomics, including gut microbiome, gastrocnemius metabolome, and proteome.

The concept of the gut−muscle axis represents a novel development in the fields of nutrition and sports medicine. Recent investigations from both animal and human studies have illuminated gut microbiota can affect the host's muscle mass and function.[25,26] Moreover, lack of gut microbiota has been linked to skeletal muscle damage, whereas the restoration of both mouse and healthy human microbiota has shown potential for restoring muscle function.[27,28] Many studies have found that the regulation of gut microbiota as a potential therapeutic strategy for sarcopenia based on gut−muscle axis.[14,29]

Our data reveal that the administration of DP ameliorates sarcopenia in STZ-induced SAMP8 mice by regulating the gut microbiota composition. DP reduced the Parabacteroides, and Enterobacteriaceae, while it increased Lachnospiraceae_NK4A136 in diabetic mice. Lee et al. reported that the content of Parabacteroides and Enterobacteriaceae significantly increased among sarcopenic patients.[30] Enterobacteriaceae was negatively correlated with muscle mass.[16] Lachnospiraceae, a normal gut microbiota, was significant diminished in cancer

https://doi.org/10.1021/acs.jafc.4c03929
J. Agric. Food Chem. XXXX, XXX, XXX−XXX

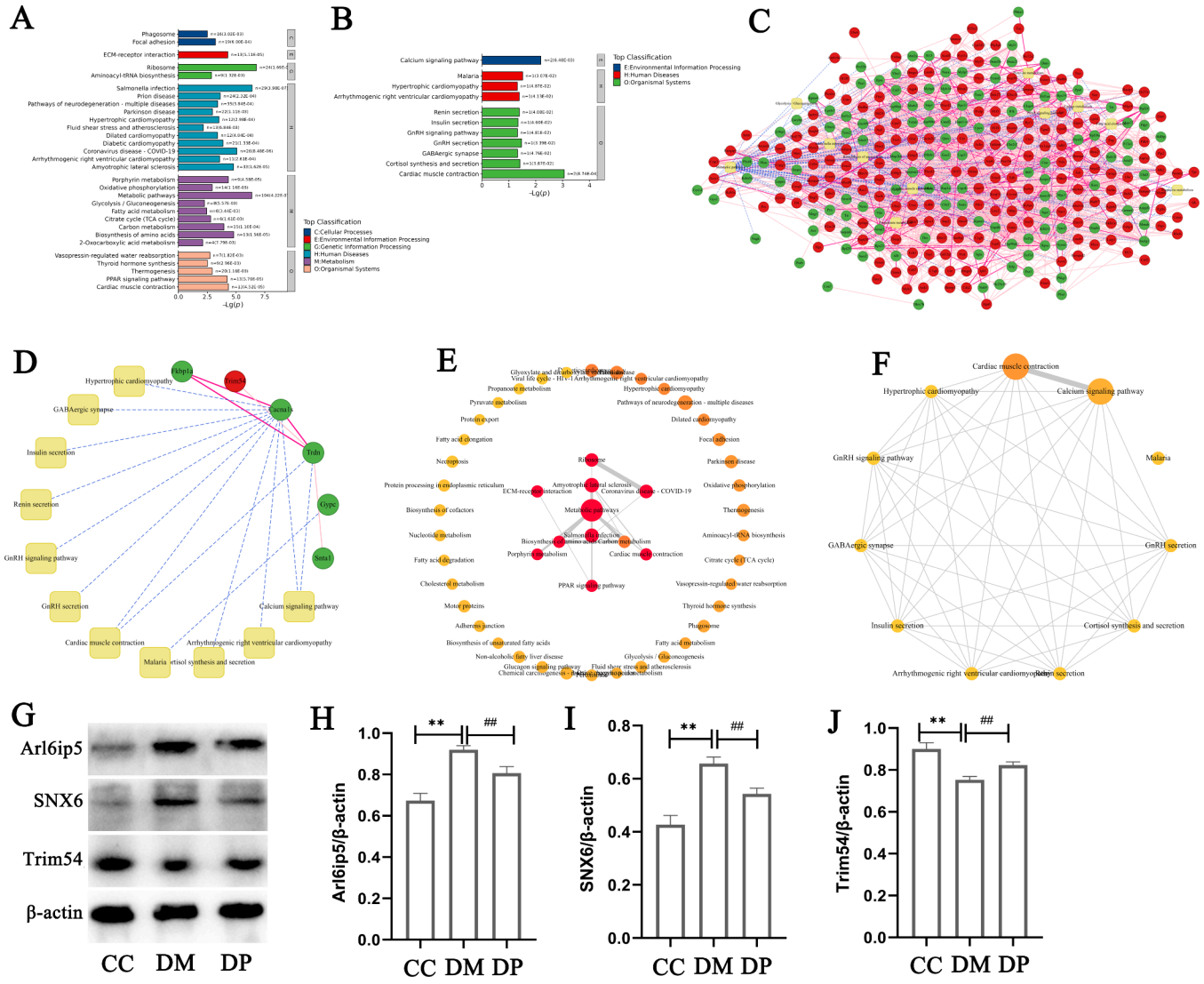

Figure 7. KEGG pathway enrichment and PPI network analysis, validation of DP targets of proteomics with Western blot. KEGG signaling pathways of differential expression proteins: (A) between DM group and CC group, (B) between DP group and DM group. PPI pathway−gene network: (C) between DM group and CC group; (D) between DP group and DM group. PPI pathway−pathway network: (E) between DM group and CC group; (F) between DP group and DM group. (G) A, Western blot images of Arl6ip5, SNX6, and Trim54 in the gastrocnemius tissue. (H–J) Data were expressed as the expression ratio of Arl6ip5/β-actin, SNX6/β-actin, and Trim54/β-actin. $^{*}P < 0.05$, $^{**}P < 0.01$ compared with CC group; $^{\#}P < 0.05$, $^{\#\#}P < 0.01$ compared with DM group. CC, control SAMP8 group; DM, STZ induced SAMP8 group; DP, DP treated STZ induced SAMP8 group. DP, D-pinitol.

cachexia mice.[31] Our results suggested that the regulation of gut microbiota by DP partly contributed to the improvement of DS.

Among the identified metabolites, carnosine, His, 5′-UMP, and 5′-CMP decreased in the gastrocnemius of STZ-induced SAMP8 mice and were restored by DP treatment. Carnosine, mainly found in skeletal muscle, is synthesized by carnosine synthetase from β-alanine and His. It plays a crucial role in pH homeostasis and increases muscle strength by enhancing the sarcomere's sensitivity to calcium. The concentrations of carnosine become depleted in sarcopenia.[32,33] His, an essential amino acid, is not only vital for treating various diseases and providing tissue protection but also as a supplement to improve muscle performance.[34] Kumar et al. reported that salbutamol could ameliorate skeletal muscle atrophy in diabetic rats by restoring the His-to-tyrosine ratio and inhibiting the pro-inflammatory cytokines.[35] Moreover, 5′-UMP and 5′-CMP can promote myogenic differentiation and mitochondrial biogenesis and reduce muscular atrophy.[36,37] Our results suggested that the restoration of the carnosine, His, 5′-UMP, and 5′-CMP by DP treatment significantly contributes to the improvement of DS.

ARL6IP5 (also known as addicin in mice, glutamate transporter associated protein 3-18 (GTRAP3-18) in rats, and JWA in humans) is a member of the prenylated Rab receptor (PRA) 1 domain family and a multifunctional physiological and pathological regulatory factor with widespread expression in tissues, including the skeletal muscle, heart, brain, and kidney.[38] Moreover, it plays an important role in cell differentiation regulation, amino acid metabolism, cytoskeleton formation, DNA damage and repair, oxidative stress, cell proliferation, and apoptosis.[39] Barbagallo reported that the transcription factor CEBPA is an important regulatory factor in islets β apoptosis through regulated the ARL6IP5

https://doi.org/10.1021/acs.jafc.4c03929
J. Agric. Food Chem. XXXX, XXX, XXX−XXX

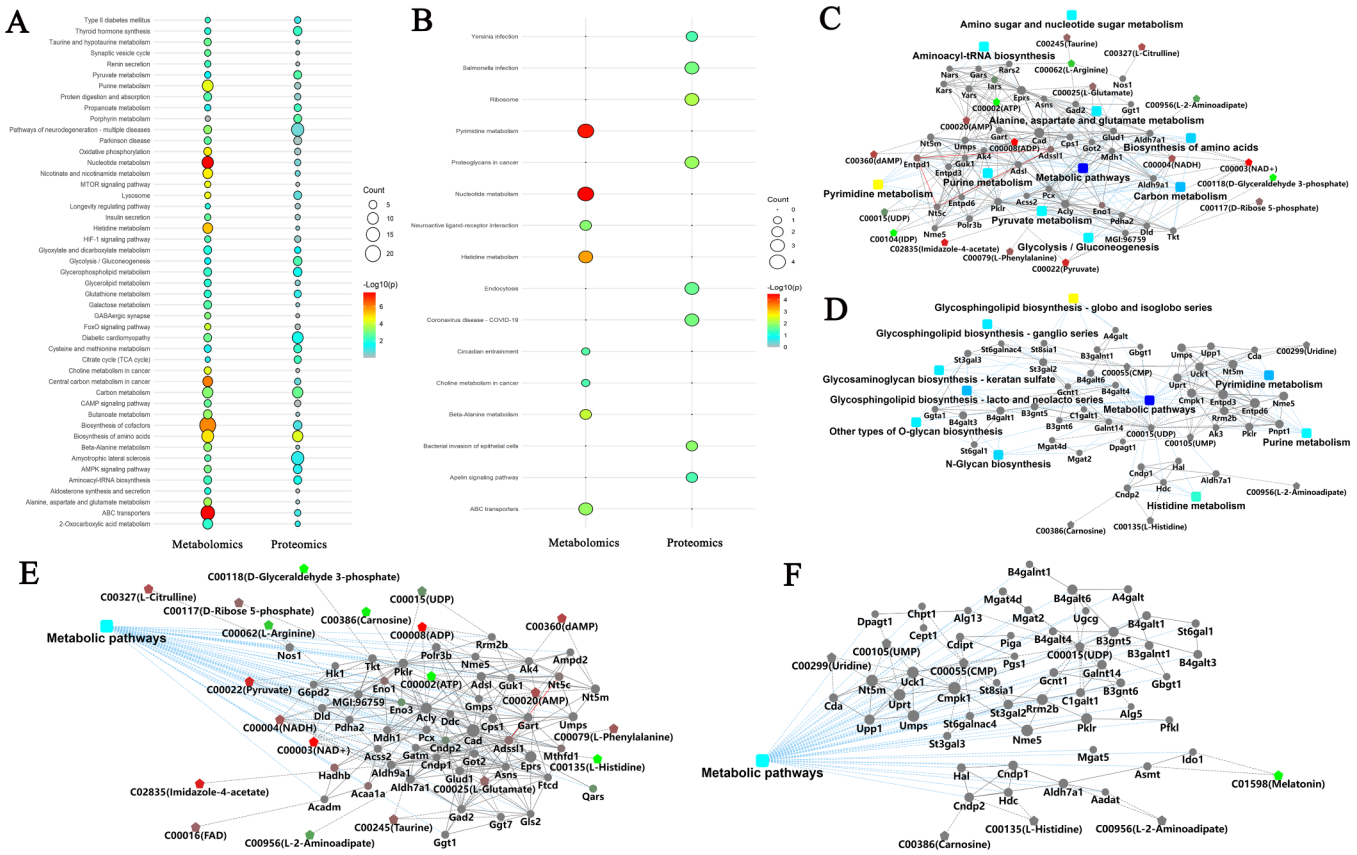

Figure 8. Associations between metabolome and proteome. KEGG signaling pathways of DRMs-DEPs: (A) between DM group and CC group, (B) between DP group and DM group. Overview of PPI network of DRMs-DEPs: (C) between DM group and CC group, (D) between DP group and DM group. Metabolic pathways of PPI network of DRMs-DEPs: (E) between DM group and CC group, (F) between DP group and DM group. CC, control SAMP8 group; DM, STZ induced SAMP8 group; DP, DP treated STZ induced SAMP8 group. DRMs, differentially regulated metabolites; DRPs, differentially expressed proteins; DP, D-pinitol.

function.[40] GTRAP3-18 regulates glutamate transport as a negative regulator of EAAT3 function.[41] Glutamate is not only crucial for energy metabolism, amino acid transport, protein biosynthesis, and neurotransmitter transmission but also has been identified as a biomarker and potential therapeutic target for sarcopenia in type 2 diabetes patients.[42] Furthermore, our results found that DP increased the expression of Trim54 protein in the gastrocnemius of diabetic mice. Trim54 is known to be a significant player in anti-inflammation and antiapoptosis.[43] Heterozygous Trim54 mutations and homozygous Trim63 play important roles in severe cardiomyopathy and skeletal muscle disease.[44] These proteins provide new insights into DS therapeutic targets.

The correlation analysis has revealed a significant association between gut microbiota (Parabacteroides, Akkermansia, Lachnospiraceae) and gastrocnemius metabolites (carnosine, 5′-UMP, 5′-CMP), indicating that the gut−muscle axis is instrumental in the pathogenesis of DS. Moreover, the common pathway between metabolome and proteome consisted of β-alanine, His, purine, pyrimidine metabolism, and ABC transporters. β-Alanine is the main metabolite of β-alanine metabolism, which is absorbed by skeletal muscles and combines with His to form carnosine. Furst et al. reported that β-alanine supplementation could improve muscle strength in the elderly.[33] His metabolism is another important pathway closely related to sarcopenia. ABC transporters, a family of membrane proteins, are involved in many crucial physiological processes, including those related to DS.[45,46] Beyond gut microbiota and host gastrocnemius metabolite interactions, the integrated analysis of DRMs-DEPs provided new insights into the mechanism of DS and therapeutic targets of DP.

In conclusion, our study established the relationship between gut microbiota, gastrocnemius metabolites, and proteins in the STZ induced SAMP8 mice treated with or without DP. DP treatment can improve sarcopenia by regulating the gut microbiota, metabolites, and proteins in diabetic mice. The protective mechanism is mainly related to β-alanine, His metabolism, ABC transporters, and the calcium signaling pathway. This study verified the important role of the gut−muscle axis in the pathogenesis of DS. The effectiveness of DP in this study provides a rationale for its clinical application and offers a theoretical basis for the development of new treatments targeting these pathways to improve outcomes for patients with DS.

■ ASSOCIATED CONTENT

Supporting Information

The Supporting Information is available free of charge at https://pubs.acs.org/doi/10.1021/acs.jafc.4c03929.

Diabetic mice model; detailed metabolomics, proteomics, and bioinformatic analysis; DP treatment restored gut microbiota, metabolites, and proteins; KEGG pathway of metabolites and proteins; principal component analysis and permutation test of metabolomics;

https://doi.org/10.1021/acs.jafc.4c03929
J. Agric. Food Chem. XXXX, XXX, XXX−XXX

PCA plots of proteomics; integrated analysis of gut microbiome, and metabolome (PDF)

Accession Codes

The mass spectrometry proteomics data are available from the ProteomeXchange Consortium (PXD048486).

AUTHOR INFORMATION

Corresponding Authors

Xiaoli Li − *Department of Pharmacy, Qilu Hospital of Shandong University, Jinan 250012, China;* orcid.org/0000-0001-5919-6181; Email: lixiaoli@email.sdu.edu.cn

Mei Cheng − *Department of Geriatric Medicine, Qilu Hospital of Shandong University, Jinan 250012, China; Key Laboratory of Cardiovascular Proteomics of Shandong Province, Qilu Hospital of Shandong University, Jinan 250012, China; Jinan Clinical Research Center for Geriatric Medicine (202132001), Jinan 250012, China;* Email: jncm65@email.sdu.edu.cn

Authors

Xin Yu − *Department of Geriatric Medicine, Qilu Hospital of Shandong University, Jinan 250012, China; Key Laboratory of Cardiovascular Proteomics of Shandong Province, Qilu Hospital of Shandong University, Jinan 250012, China; Jinan Clinical Research Center for Geriatric Medicine (202132001), Jinan 250012, China*

Pei Li − *Department of Respiratory Medicine, Shandong Cancer Hospital and Institute, Shandong First Medical University and Shandong Academy of Medical Sciences, Jinan 250117, China*

Baoying Li − *Health Management Center (East Area), Qilu Hospital of Shandong University, Jinan 250101, China;* orcid.org/0000-0002-5845-0720

Fei Yu − *Department of Geriatric Medicine, Qilu Hospital of Shandong University, Jinan 250012, China; Key Laboratory of Cardiovascular Proteomics of Shandong Province, Qilu Hospital of Shandong University, Jinan 250012, China; Jinan Clinical Research Center for Geriatric Medicine (202132001), Jinan 250012, China*

Wenqian Zhao − *Department of Geriatric Medicine, Qilu Hospital of Shandong University, Jinan 250012, China; Key Laboratory of Cardiovascular Proteomics of Shandong Province, Qilu Hospital of Shandong University, Jinan 250012, China; Jinan Clinical Research Center for Geriatric Medicine (202132001), Jinan 250012, China*

Xue Wang − *Department of Geriatric Medicine, Qilu Hospital of Shandong University, Jinan 250012, China; Key Laboratory of Cardiovascular Proteomics of Shandong Province, Qilu Hospital of Shandong University, Jinan 250012, China; Jinan Clinical Research Center for Geriatric Medicine (202132001), Jinan 250012, China*

Yajuan Wang − *Department of Geriatric Medicine, Qilu Hospital of Shandong University, Jinan 250012, China; Key Laboratory of Cardiovascular Proteomics of Shandong Province, Qilu Hospital of Shandong University, Jinan 250012, China; Jinan Clinical Research Center for Geriatric Medicine (202132001), Jinan 250012, China*

Haiqing Gao − *Department of Geriatric Medicine, Qilu Hospital of Shandong University, Jinan 250012, China; Key Laboratory of Cardiovascular Proteomics of Shandong Province, Qilu Hospital of Shandong University, Jinan 250012, China; Jinan Clinical Research Center for Geriatric Medicine (202132001), Jinan 250012, China*

Complete contact information is available at: https://pubs.acs.org/10.1021/acs.jafc.4c03929

Author Contributions

X.Y., P.L., and B.L. wrote the manuscript. X.Y., P.L., B.L., F.Y., W.Z., X.W., and Y.W. performed the experiments. X.Y., X.L., P.L., M.C., and B.L. prepared figures and acquired data. H.G., M.C. and X.L. reviewed and edited the manuscript. All authors have read and agreed to the published version of the manuscript.

Notes

The authors declare no competing financial interest.

ACKNOWLEDGMENTS

This work was supported by Natural Science Foundation of Shandong Province (ZR2021MH376). We thank Hong Yu and Xianggan Cui of Shanghai Bioprofile Biotechnology Co., Ltd.

ABBREVIATIONS

Arl6ip5, ADP ribosylation factor-like GTPase 6 interacting protein 5; 5′-CMP, cytidine 5′-monophosphate; DEPs, differentially expressed proteins; DP, D-pinitol; DRMs, differentially regulated metabolites; DS, diabetic sarcopenia; FBG, fasting blood glucose; His, histidine; SNX 6, sorting nexins 6; Trim54, tripartite motif containing protein 54; 5′-UMP, uridine 5′-monophosphate

REFERENCES

(1) Aluganti Narasimhulu, C.; Singla, D. K. Amelioration of diabetes-induced inflammation mediated pyroptosis, sarcopenia, and adverse muscle remodelling by bone morphogenetic protein-7. *J. Cachexia. Sarcopenia. Muscle.* **2021**, *12*, 403−420.

(2) Mesinovic, J.; Fyfe, J. J.; Talevski, J.; Wheeler, M. J.; Leung, G. K. W.; George, E. S.; Hunegnaw, M. T.; Glavas, C.; Jansons, P.; Daly, R. M.; et al. Type 2 Diabetes Mellitus and Sarcopenia as Comorbid Chronic Diseases in Older Adults: Established and Emerging Treatments and Therapies. *Diabetes. Metab. J.* **2023**, *47*, 719−742.

(3) Muvhulawa, N.; Mazibuko-Mbeje, S. E.; Ndwandwe, D.; Silvestri, S.; Ziqubu, K.; Moetlediwa, M. T.; Mthembu, S. X. H.; Marnewick, J. L.; Van der Westhuizen, F. H.; Nkambule, B. B.; et al. Sarcopenia in a type 2 diabetic state: Reviewing literature on the pathological consequences of oxidative stress and inflammation beyond the neutralizing effect of intracellular antioxidants. *Life. Sci.* **2023**, *332*, 122125.

(4) Feng, L.; Gao, Q.; Hu, K.; Wu, M.; Wang, Z.; Chen, F.; Mei, F.; Zhao, L.; Ma, B. Prevalence and Risk Factors of Sarcopenia in Patients With Diabetes: A Meta-analysis. *J. Clin. Endocrinol. Metab.* **2022**, *107*, 1470−1483.

(5) Zhang, X.; Zhao, Y.; Chen, S.; Shao, H. Anti-diabetic drugs and sarcopenia: emerging links, mechanistic insights, and clinical implications. *J. Cachexia. Sarcopenia. Muscle.* **2021**, *12*, 1368−1379.

(6) Wang, T.; Xu, H.; Wu, S.; Guo, Y.; Zhao, G.; Wang, D. Mechanisms Underlying the Effects of the Green Tea Polyphenol EGCG in Sarcopenia Prevention and Management. *J. Agric. Food. Chem.* **2023**, *71*, 9609−9627.

(7) Lee, D. Y.; Chun, Y. S.; Kim, J. K.; Lee, J. O.; Ku, S. K.; Shim, S. M. Curcumin Attenuates Sarcopenia in Chronic Forced Exercise Executed Aged Mice by Regulating Muscle Degradation and Protein Synthesis with Antioxidant and Anti-inflammatory Effects. *J. Agric. Food. Chem.* **2021**, *69*, 6214−6228.

(8) Choi, P. G.; Park, S. H.; Jeong, H. Y.; Kim, H. S.; Hahm, J. H.; Seo, H. D.; Ahn, J.; Jung, C. H. Geniposide attenuates muscle atrophy via the inhibition of FoxO1 in senescence-accelerated mouse prone-8. *Phytomedicine.* **2024**, *123*, 155281.

(9) Li, X. L.; Xu, M.; Yu, F.; Fu, C. L.; Yu, X.; Cheng, M.; Gao, H. Q. Effects of D-pinitol on myocardial apoptosis and fibrosis in streptozocin-induced aging-accelerated mice. *J. Food. Biochem.* **2021**, *45*, No. e13669.
(10) Li, X. L.; Yu, F.; Fu, C. L.; Yu, X.; Xu, M.; Cheng, M. Phosphoproteomics analysis of diabetic cardiomyopathy in aging-accelerated mice and effects of D-pinitol. *Proteomics. Clin. Appl.* **2022**, *16*, No. e2100019.
(11) Kang, M. J.; Kim, J. I.; Yoon, S. Y.; Kim, J. C.; Cha, I. J. Pinitol from soybeans reduces postprandial blood glucose in patients with type 2 diabetes mellitus. *J. Med. Food.* **2006**, *9*, 182−186.
(12) Kim, H. J.; Park, K. S.; Lee, S. K.; Min, K. W.; Han, K. A.; Kim, Y. K.; Ku, B. J. Effects of pinitol on glycemic control, insulin resistance and adipocytokine levels in patients with type 2 diabetes mellitus. *Ann. Nutr. Metab.* **2012**, *60*, 1−5.
(13) Zhang, C.; Wu, W.; Xin, X.; Li, X.; Liu, D. Extract of ice plant (Mesembryanthemum crystallinum) ameliorates hyperglycemia and modulates the gut microbiota composition in type 2 diabetic Goto-Kakizaki rats. *Food. Funct.* **2019**, *10*, 3252−3261.
(14) Liu, Y.; Guo, Y.; Liu, Z.; Feng, X.; Zhou, R.; He, Y.; Zhou, H.; Peng, H.; Huang, Y. Augmented temperature fluctuation aggravates muscular atrophy through the gut microbiota. *Nat. Commun.* **2023**, *14*, 3494.
(15) Lefevre, C.; Bindels, L. B. Role of the Gut Microbiome in Skeletal Muscle Physiology and Pathophysiology. *Curr. Osteoporos. Rep.* **2022**, *20*, 422−432.
(16) Zhang, Y.; Zhu, Y.; Guo, Q.; Wang, W.; Zhang, L. High-throughput sequencing analysis of the characteristics of the gut microbiota in aged patients with sarcopenia. *Exp. Gerontol.* **2023**, *182*, 112287.
(17) Chen, H.; Huang, X.; Dong, M.; Wen, S.; Zhou, L.; Yuan, X. The Association Between Sarcopenia and Diabetes: From Pathophysiology Mechanism to Therapeutic Strategy. Diabetes. *Metab. Syndr. Obes.* **2023**, *16*, 1541−1554.
(18) Okamura, T.; Hamaguchi, M.; Nakajima, H.; Kitagawa, N.; Majima, S.; Senmaru, T.; Okada, H.; Ushigome, E.; Nakanishi, N.; Sasano, R.; et al. Milk protects against sarcopenic obesity due to increase in the genus Akkermansia in faeces of db/db mice. *J. Cachexia. Sarcopenia. Muscle.* **2023**, *14*, 1395−1409.
(19) He, R.; Gao, S.; Yao, H.; Zhao, Z.; Tong, J.; Zhang, H. Mechanism of Metabolic Response to Hepatectomy by Integrated Analysis of Gut Microbiota, Metabolomics, and Proteomics. *Microbiol. Spectr.* **2023**, *11*, No. e02067-22.
(20) Li, X.; Yu, X.; Gao, Y.; Zhao, W.; Wang, Y.; Yu, F.; Fu, C.; Gao, H.; Cheng, M.; Li, B. TMT proteomics analysis reveals the mechanism of bleomycin-induced pulmonary fibrosis and effects of Ginseng honeysuckle superfine powdered tea. *Chin. Med.* **2023**, *18*, 60.
(21) Giha, H. A.; Alamin, O. A. O.; Sater, M. S. Diabetic sarcopenia: metabolic and molecular appraisal. *Acta. Diabetol.* **2022**, *59*, 989−1000.
(22) She, M.; Huang, M.; Zhang, J.; Yan, Y.; Zhou, L.; Zhang, M.; Yang, Y.; Wang, D. Astragulus embranaceus (Fisch.) Bge-Dioscorea opposita Thunb herb pair ameliorates sarcopenia in senile type 2 diabetes mellitus through Rab5a/mTOR-mediated mitochondrial dysfunction. *J. Ethnopharmacol.* **2023**, *317*, 116737.
(23) Yoshimura, Y.; Hashimoto, Y.; Okada, H.; Takegami, M.; Nakajima, H.; Miyoshi, T.; Yoshimura, T.; Yamazaki, M.; Hamaguchi, M.; Fukui, M. Changes in glycemic control and skeletal muscle mass indices after dapagliflozin treatment in individuals with type 1 diabetes mellitus. *J. Diabetes. Investig.* **2023**, *14*, 1175−1182.
(24) Yan, S. B.; Liang, H.; Zhan, P.; Zheng, H.; Zhao, Q. X.; Zheng, Z. J.; Lu, H. X.; Shang, G. K.; Ji, X. P. Stimulator of interferon genes promotes diabetic sarcopenia by targeting peroxisome proliferator activated receptors γ degradation and inhibiting fatty acid oxidation. *J. Cachexia. Sarcopenia. Muscle.* **2023**, *14*, 2623−2641.
(25) Lee, J. Y.; Shin, S. K.; Bae, H. R.; Ji, Y.; Park, H. J.; Kwon, E. Y. The animal protein hydrolysate attenuates sarcopenia via the muscle-gut axis in aged mice. *Biomed. Pharmacother.* **2023**, *167*, 115604.
(26) Daily, J. W.; Park, S. Sarcopenia Is a Cause and Consequence of Metabolic Dysregulation in Aging Humans: Effects of Gut Dysbiosis, Glucose Dysregulation, Diet and Lifestyle. *Cells.* **2022**, *11*, 338.
(27) Chen, L. H.; Chang, S. S.; Chang, H. Y.; Wu, C. H.; Pan, C. H.; Chang, C. C.; Chan, C. H.; Huang, H. Y. Probiotic supplementation attenuates age-related sarcopenia via the gut-muscle axis in SAMP8 mice. *J. Cachexia. Sarcopenia. Muscle.* **2022**, *13*, 515−531.
(28) Liao, X.; Wu, M.; Hao, Y.; Deng, H. Exploring the Preventive Effect and Mechanism of Senile Sarcopenia Based on ″Gut-Muscle Axis″. *Front. Bioeng. Biotechnol.* **2020**, *8*, 590869.
(29) Mancin, L.; Wu, G. D.; Paoli, A. Gut microbiota-bile acid-skeletal muscle axis. *Trends. Microbiol.* **2023**, *31*, 254−269.
(30) Lee, Y. A.; Song, S. W.; Jung, S. Y.; Bae, J.; Hwang, N.; Kim, H. N. Sarcopenia in community-dwelling older adults is associated with the diversity and composition of the gut microbiota. *Exp. Gerontol.* **2022**, *167*, 111927.
(31) Feng, L.; Zhang, W.; Shen, Q.; Miao, C.; Chen, L.; Li, Y.; Gu, X.; Fan, M.; Ma, Y.; Wang, H.; et al. Bile acid metabolism dysregulation associates with cancer cachexia: roles of liver and gut microbiome. *J. Cachexia. Sarcopenia. Muscle.* **2021**, *12*, 1553−1569.
(32) Zhao, Q.; Shen, H.; Liu, J.; Chiu, C. Y.; Su, K. J.; Tian, Q.; Kakhniashvili, D.; Qiu, C.; Zhao, L. J.; Luo, Z.; et al. Pathway-based metabolomics study of sarcopenia- related traits in two US cohorts. *Aging.* **2022**, *14*, 2101−2112.
(33) Furst, T.; Massaro, A.; Miller, C.; Williams, B. T.; LaMacchia, Z. M.; Horvath, P. J. β-Alanine supplementation increased physical performance and improved executive function following endurance exercise in middle aged individuals. *J. Int. Soc. Sports. Nutr.* **2018**, *15*, 32.
(34) Holeček, M. Influence of Histidine Administration on Ammonia and Amino Acid Metabolism: A Review. *Physiol. Res.* **2020**, *69*, 555−564.
(35) Kumar, A.; Prajapati, P.; Singh, G.; Kumar, D.; Mishra, V.; Kim, S. C.; Raorane, C. J.; Raj, V.; Kushwaha, S. Salbutamol Attenuates Diabetic Skeletal Muscle Atrophy by Reducing Oxidative Stress, Myostatin/GDF-8, and Pro-Inflammatory Cytokines in Rats. *Pharmaceutics.* **2023**, *15*, 2101.
(36) Mamedova, L. K.; Wang, R.; Besada, P.; Liang, B. T.; Jacobson, K. A. Attenuation of apoptosis in vitro and ischemia/reperfusion injury in vivo in mouse skeletal muscle by P2Y6 receptor activation. *Pharmacol. Res.* **2008**, *58*, 232−239.
(37) Nakagawara, K.; Takeuchi, C.; Ishige, K. 5′-CMP and 5′-UMP alleviate dexamethasone-induced muscular atrophy in C2C12 myotubes. *Biochem. Biophys. Rep.* **2023**, *34*, 101460.
(38) Akiduki, S.; Ochiishi, T.; Ikemoto, M. J. Neural localization of addicsin in mouse brain. *Neurosci. Lett.* **2007**, *426*, 149−154.
(39) Siddique, I.; Kamble, K.; Gupta, S.; Solanki, K.; Bhola, S.; Ahsan, N.; Gupta, S. ARL6IP5 Ameliorates α-Synuclein Burden by Inducing Autophagy via Preventing Ubiquitination and Degradation of ATG12. *Int. J. Mol. Sci.* **2023**, *24*, 10499.
(40) Barbagallo, D.; Condorelli, A. G.; Piro, S.; Parrinello, N.; Fløyel, T.; Ragusa, M.; Rabuazzo, A. M.; Størling, J.; Purrello, F.; Di Pietro, C.; et al. CEBPA exerts a specific and biologically important proapoptotic role in pancreatic β cells through its downstream network targets. *Mol. Biol. Cell* **2014**, *25*, 2333−2341.
(41) Butchbach, M. E.; Lai, L.; Lin, C. L. Molecular cloning, gene structure, expression profile and functional characterization of the mouse glutamate transporter (EAAT3) interacting protein GTRAP3−18. *Gene.* **2002**, *292*, 81−90.
(42) Nakajima, H.; Okada, H.; Kobayashi, A.; Takahashi, F.; Okamura, T.; Hashimoto, Y.; Nakanishi, N.; Senmaru, T.; Ushigome, E.; Hamaguchi, M.; et al. Leucine and Glutamic Acid as a Biomarker of Sarcopenic Risk in Japanese People with Type 2 Diabetes. *Nutrients.* **2023**, *15*, 2400.
(43) Chen, H.; Chen, X.; Yang, L.; Sheng, S.; Yang, J.; Lu, Y.; Sun, Y.; Zhang, X.; Jiang, C. TRIM54 alleviates inflammation and apoptosis by stabilizing YOD1 in rat tendon-derived stem cells. *J. Biol. Chem.* **2024**, *300*, 105510.

https://doi.org/10.1021/acs.jafc.4c03929
J. Agric. Food Chem. XXXX, XXX, XXX−XXX

(44) Olivé, M.; Abdul-Hussein, S.; Oldfors, A.; González-Costello, J.; van der Ven, P. F.; Fürst, D. O.; González, L.; Moreno, D.; Torrejón-Escribano, B.; Alió, J.; et al. New cardiac and skeletal protein aggregate myopathy associated with combined MuRF1 and MuRF3 mutations. *Hum. Mol. Genet.* **2015**, *24*, 6264.
(45) Zhou, J.; Liu, J.; Lin, Q.; Shi, L.; Zeng, Z.; Guan, L.; Ma, Y.; Zeng, Y.; Zhong, S.; Xu, L. Characteristics of the gut microbiome and metabolic profile in elderly patients with sarcopenia. *Front. Pharmacol.* **2023**, *14*, 1279448.
(46) Tan, Y.; Liu, X.; Yang, Y.; Li, B.; Yu, F.; Zhao, W.; Fu, C.; Yu, X.; Han, Z.; Cheng, M. Metabolomics analysis reveals serum biomarkers in patients with diabetic sarcopenia. *Front. Endocrinol (Lausanne).* **2023**, *14*, 1119782.

https://doi.org/10.1021/acs.jafc.4c03929
J. Agric. Food Chem. XXXX, XXX, XXX−XXX